Journal of the European Ceramic Society 16 (1996) 819–824

S0955-2219(96)00002-7
0955-2219/96/$15.00 +.00

Cathodic Electrosynthesis of Ceramic Deposits

I. Zhitomirsky & L. Gal-Or

Israel Institute of Metals, Technion-Israel Institute of Technology, Haifa, 32000, Israel

(Received 10 October 1995; revised version received 28 November 1995; accepted 5 December 1995)

Abstract

Cathodic electrosynthesis of TiO_2, ZrO_2 and $ZrTiO_4$ deposits on platinum substrates was performed via hydrolysis of $TiCl_4$ and $ZrOCl_2$ salts dissolved in a mixed methanol–water solvent in presence of hydrogen peroxide by an electrogenerated base. The deposits were characterized by XRD, TG/DTA, SEM and EDS. Deposits as obtained were amorphous. The crystallization behaviour of the deposits has been studied. Crystallite sizes were derived at different temperatures from X-ray broadening data. A possible mechanism of electrosynthesis and the role of hydrogen peroxide are discussed.

1 Introduction

A cathodic electrodeposition process has recently enabled the formation of films of different ceramic materials. These materials encompass individual oxides (Al_2O_3, ZrO_2, CeO_2, PbO *et al.*[1–7]) as well as complex compounds, including ferroelectric materials ($BaTiO_3$ and PZT[8,9]), high temperature superconductors ($YBa_2Cu_3O_{7-x}$[10,11]), and biomaterials.[12,13] Cathodic electrodeposition is achieved via hydrolysis of metal ions by an electrogenerated base to form metal oxide/hydroxide films on the cathodic substrate. Different chemical reactions available for the generation of base were discussed in literature.[1,3] It should be noted that reduction of water and nitrate are important cathodic reactions used for the electrodeposition process. However, the electrodeposition of titania in this way presents difficulties. The titanium nitrate salt is an unstable compound and is not available commercially. Difficulties are also associated with the use of other inorganic salts of Ti^{4+} in aqueous solutions since they are easily hydrolyzed in water to form a titanium hydroxide precipitate. Matsumoto and coworkers used $TiCl_3$ salt for electrodeposition.[8,9] They suggested that Ti^{3+} ions do not exist in the solution since they transform to Ti^{4+} or TiO^{2+}.[8,9] In their experiments on electrodeposition of important ferroelectric materials such as $BaTiO_3$ and PZT difficulties were encountered with the control of deposit stoichiometry due to different deposition rates of individual components. No deposition was achieved by the authors on platinum substrates. It should be noted that electrodeposition holds important perspectives for the development of various ferroelectric thin film devices. Since titanates constitute one of the important groups of ferroelectric materials currently used in industry, it is important to develop an electrodeposition process for formation of titania and stoichiometric complex titanates on platinum substrates.

In previous works,[14,15] a novel approach has been advanced for the electrodeposition of oxide films. The problem of titania electrodeposition was solved by use of a peroxocomplex[16] of titanium instead of titanium ions. The peroxocomplex of titanium is stable under certain conditions in aqueous solutions,[16] therefore water can be used as a solvent and a source of OH^- groups which are necessary for the deposition process. Deposition was performed from mixed *N,N*-Dimethylformamide(DMF)–water solutions.[14] It was pointed out that non-aqueous solvents are preferable for morphology optimization, however the deposition process needs certain amounts of water for base generation and for prevention of formation of non-stoichiometric titania. Deposition of titania was achieved via hydrolysis of the peroxocomplex by electrogenerated base and thermal decomposition of the obtained deposit (hydrated peroxocompound). This approach has been further expanded to formation of complex compounds. $ZrTiO_4$ has been deposited on graphite from a mixed water–methanol solvent.[15] It was established that the use of a peroxoprecursor provides equal deposition rates of the individual components and allows to obtain a deposit of desired stoichiometry. However, the exact mechanism of $ZrTiO_4$ electrodeposition is not fully understood. The purpose of this work is to study the deposition of titania, zirconia and $ZrTiO_4$ on platinum substrates and to get a better understanding of the mechanism of deposition via peroxoprecursors.

2 Experimental Procedures

As starting materials commercially guaranteed salts of $TiCl_4$, $ZrOCl_2 \cdot 8H_2O$ and hydrogen peroxide H_2O_2 (30 wt% in water) were used. Three different solutions in a mixed methanol–water (3:1 volume ratio) solvent were prepared. Stock solution 1 contained 0·005 M $TiCl_4$ and hydrogen peroxide additive in a ratio of $TiCl_4$:H_2O_2 = 1:1·2. Stock solution 2 contained 0·005 M $ZrOCl_2$ and hydrogen peroxide, $ZrOCl_2$:H_2O_2 = 1:1·2. For preparation of stock solution 3 reagents were mixed in a ratio $ZrOCl_2$:$TiCl_4$:H_2O_2 = 1:1:2·4, total concentration of $ZrOCl_2$ and $TiCl_4$ was 0·005 M. Rectangular Pt specimens (40 × 15 × 0·1 mm) were used as cathodic substrates. The electrochemical cell for deposition in a galvanostatic regime included the cathodic substrate centered between two parallel platinum counterelectrodes. Electrodeposition experiments were performed at 1°C. Cathodic deposits were obtained at a constant current density of 20 mA/cm^2. Deposition times were in the range of up to 20 min. After drying at room temperature deposits were removed from the substrates and subjected to X-ray and TG/DTA study. The phase content was determined by X-ray diffraction with a diffractometer (Phillips, PW-1820) using monochromatized CuK_α radiation. The Scherrer relationship

$$D = \frac{0{\cdot}9\ \lambda}{\beta \cos\theta}$$

was used for calculation of the crystallite size from X-ray line broadening measurements, where D is the average crystallite size, λ is the X-ray wave length, β is the full width at half maximum of the peak and θ is the Bragg angle. A commercially available computer program has been utilized for the profile fitting procedure. Correction for instrumental broadening has been performed. Thermal analysis was carried out in air between room temperature and 800°C at a heating rate of 10°C/min using a thermoanalyzer (Setaram, TGA92). The microstructure of the obtained deposits was studied using a scanning electron microscope (Jeol, JSM-840) equipped with EDS. EDS studies were performed on powder specimens which were obtained by removing green deposits from the substrates and annealing them in air at 800°C for 1 h.

3 Results

Performed experiments revealed the formation of deposits from all the stock solutions used. X-ray analysis was made on fresh deposits and those thermally treated in air at different temperatures for 1 h. The X-ray diffractograms of fresh deposits exhibit their amorphous nature (Figs 1, 2 and 3). Results of X-ray studies of deposits obtained from stock solution 1 (deposits 1) show that faint peaks of the anatase phase appear at 300°C. In Fig. 1 it can be seen that deposit 1 thermally treated at 400°C displayed anatase peaks, which are broadened due to the fine size of the crystallites. Deposits 1 heated at higher temperatures possess an anatase structure up to 700°C. Further increase of the annealing temperature results in an anatase–rutile

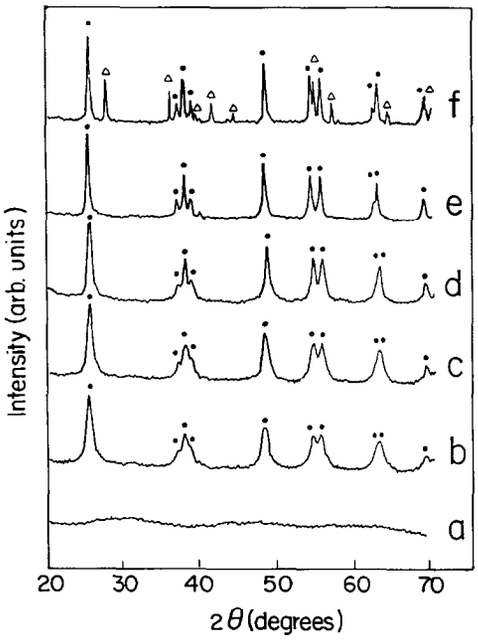

Fig. 1. X-ray diffraction patterns of deposits 1 obtained at a c.d. of 20 mA/cm^2: as-prepared (a) and after thermal treatment at different temperatures for 1 h: 400 (b); 500 (c); 600 (d); 700 (e) and 800 (f) °C. (• anatase, Δ rutile).

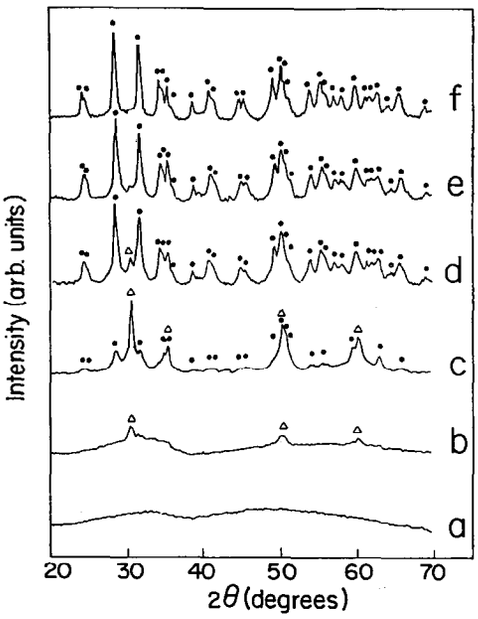

Fig. 2. X-ray diffraction patterns of deposits 2 obtained at a c.d. of 20 mA/cm^2: as-prepared (a) and after thermal treatment at different temperatures for 1 h: 400 (b); 500 (c); 600 (d); 700 (e) and 800 (f) °C. (• monoclinic zirconia, Δ tetragonal zirconia).

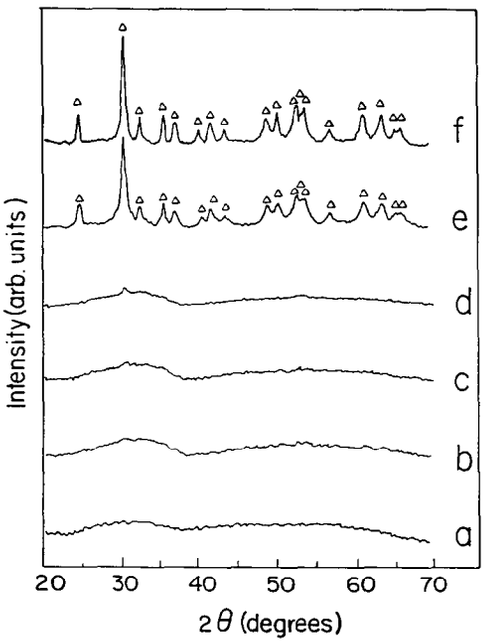

Fig. 3. X-ray diffraction patterns of deposits 3 obtained at a c.d. of 20 mA/cm^2: as-prepared (a) and after thermal treatment at different temperatures for 1 h: 400 (b); 500 (c); 600 (d); 700 (e) and 800 (f) °C (Δ $ZrTiO_4$).

transformation. Figure 1 indicates that XRD spectra taken from deposit 1 annealed at 800°C displayed reflexes of rutile in addition to those of anatase. On exposure of deposits 1 to the temperature of 1000°C, X-ray diffraction patterns exhibit only peaks of rutile. In Table 1, experimental data are given on crystallite size of deposits 1 thermally treated at different temperatures. From this table it can be seen that nanometer-sized anatase forms at 400°C and crystallite size increases with temperature. It is interesting to notice, that rutile crystallites at 800°C are significantly larger than the anatase ones from which they were derived.

Figure 2 shows XRD data for deposits obtained from stock solution 2 (deposits 2). Small reflexes appear at 400°C, which become more clear and sharp at higher temperatures. It is reasonable to attribute these peaks to tetragonal zirconia. However it should be noted that it is difficult to distinguish between the cubic and tetragonal zirconia phases owing to peak broadening. After annealing at 500 and 600°C the samples consisted of mixtures of tetragonal and monoclinic zirconia. At 600°C monoclinic zirconia is dominant, at 800°C the tetragonal phase was not detected in the XRD pattern. As is seen from Table 1, sizes of tetragonal and monoclinic crystallites are on the nanometric scale, while crystallites of the monoclinic phase at 500°C were smaller than those of the tetragonal phase.

XRD data for deposits obtained from stock solution 3 (deposits 3) are summarized in Fig. 3. Deposit crystallization was observed at temperatures exceeding 600°C. The only crystalline phase in deposits 3 thermally treated at 700 and 800°C is $ZrTiO_4$, no peaks due to individual oxides were detected. The observed *d*-values match well with the Joint Committee on Powder Diffraction Standards (JCPDS) data for this material. It is remarkable, that in the temperature region of 400–600°C deposit 3 remains amorphous, whereas crystallization of deposits 1 and 2 was detected. Data presented in Table 1 indicate formation of nanosize $ZrTiO_4$. However it should be noted again that the calculations performed in this work were based on the suggestion that small particle size is the only reason of XRD line broadening.

Figure 4 shows an assemblage of TG/DTA curves for deposits 1, 2 and 3. For deposit 1 the total weight loss in temperature region up to 800°C was about 29% of the initial sample weight, however essentially most of the weight loss occurred below 300°C. The DTA curve exhibits a broad endotherm around 130°C and an exotherm at 440°C. For deposit 2, two distinct steps in the TG curve are distinguished. A sharp reduction of sample weight was observed up to ~200°C and in the region 330–415°C, then the weight fell gradually. Weight losses at 330 and 415°C were 29 and 34% respectively, the total weight loss in the temperature region up to 800°C was 36%. Two endothermic peaks around 130 and 350°C and an exothermic

Table 1. Crystallite sizes of different phases obtained from X-ray line broadening measurements. Reflexes used for calculations are designated

Temperature (°C)	*Particle size (nm)*				
	Titania		*Zirconia*		*Zirconium titanate*
	Anatase (101)	*Rutile (110)*	*Tetragonal (111)*	*Monoclinic (11-1)*	*$ZrTiO_4$ (111)*
400	13				
450			12		
500	15		31	11	
600	20			17	
700	34			20	17
800	59	147		27	18

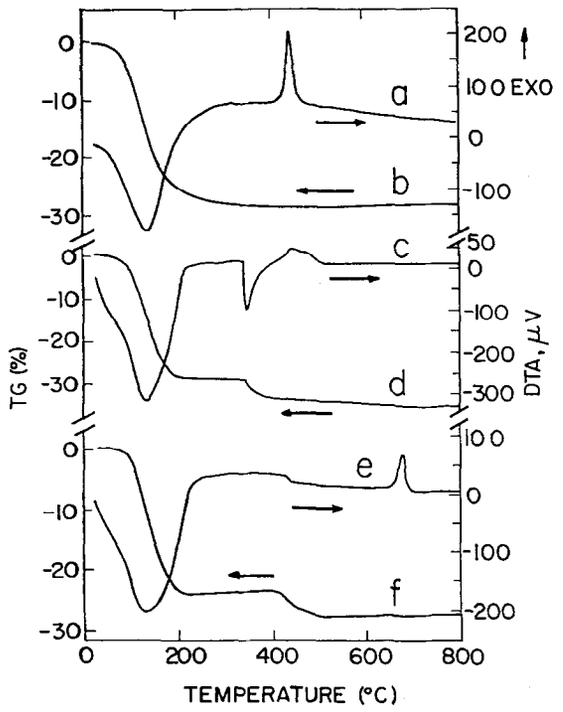

Fig. 4. DTA ((a),(c),(e)) and TG ((b),(d),(f)) data for deposits 1((a),(b)) deposits 2 ((c),(d)) and deposits 3 ((e),(f)) obtained at a 10°C/min heating rate.

effect around 460°C were observed in the DTA curve. The endothermic peak around 130°C and the exothermic peak were very broad. It is thought that the two endothermic peaks correspond to two steps in weight losses.

TG records for deposits 3 show two distinct steps in weight loss up to 200°C and in the region 410–500°C. Weight losses at 235, 540 and 800°C were 23, 27 and 28%, respectively. A very broad endotherm around ~130°C is seen in the DTA curve, a small endothermic effect could be also distinguished at ~430°C. When the specimen was heated to higher temperatures an exothermic peak at ~680°C was observed. For deposits 3, as for deposits 2, a possible link emerges between the observed endothermic effects and the steps in weight loss in corresponding temperature regions.

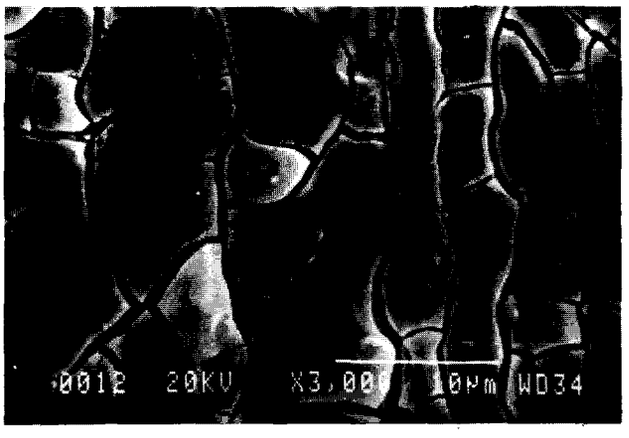

Fig. 5. SEM picture of green deposit 3 on a Pt substrate.

SEM observations indicate a fine particle structure of the deposits. A SEM picture of the green deposit 3 on a Pt substrate is shown in Fig. 5. The sample also shows cracks which arise owing to drying shrinkage. EDS data taken from 15 powder samples show the Ti/Zr ratio to be in the region 0·98–1·05.

4 Discussion

The reported results indicate that the proposed approach has no restriction with regard to platinum being used as a substrate in the deposition process. The mechanism of film formation via a peroxocomplex was discussed in previous works[14,15] and can be used to provide an explanation of the experimental data described above. It is implied that the peroxocomplex of titanium $[Ti(O_2)(OH)_{n-2}]^{(4-n)+}$ is hydrolized by the electrogenerated base to form the cathodic deposit. According to Ref. 16, below pH 1 the peroxocomplex is mononuclear, increase of the pH value causes transformation to a dinuclear and then to a polynuclear complex. Further pH increase results in precipitation of the peroxotitanium hydrate $TiO_3(H_2O)_x$. In the electrosynthesis method the high pH of the cathodic region brings about formation of a peroxotitanium hydrate, which precipitates on the electrode. The cathodic reaction that generates OH^- is:

$$2H_2O + 2e^- \Leftrightarrow H_2 + 2OH^- \quad (1)$$

The following anodic reaction occurs simultaneously:

$$2H_2O \Leftrightarrow O_2 + 4H^+ - 4e^- \quad (2)$$

Phase evolution of deposits obtained from stock solution 1 with temperature are in good agreement with Ref. 14. According to the X-ray data, crystallization of anatase was observed after thermal treatment at 400°C. It is important to note that particle size of titania is on a nanometric scale, (Table 1). This is remarkable, because nanostructured titania exhibits important properties and is now a subject of intensive investigation.[17–19] Recently it has been established that electrodeposition can be used for formation of nanostructured oxides.[2,20] Obviously, the extension of this method to titania electrodeposition is of significant interest. Crystallite sizes of electrodeposited titania at different temperatures are close to those for chemically precipitated titania.[19] A higher crystallite size of rutile than that of anatase observed at 800°C is also in agreement with Ref. 19. Observed weight losses (Fig. 4) are attributed to decomposition of the peroxocomplex and liberation of water and oxygen:

$$2TiO_3(H_2O)_x \Rightarrow 2TiO_2 + O_2 + 2xH_2O \quad (3)$$

The exothermic peak on the DTA curve at 440°C is associated with crystallization of titania.

It is reasonable to expect that in analogy to titania the formation of zirconia can be achieved via a peroxoprecursor. Indeed, according to literature,[21] the hydrated zirconium peroxide $ZrO_3(H_2O)_x$ can be precipitated from zirconium salt solutions in presence of hydrogen peroxide. However, the mechanism of zirconia deposition remains questionable taking into account $ZrO_3(H_2O)_x$ non-stability.[21] Moreover, in contrast to titania, electrodeposition of zirconia can be achieved without hydrogen peroxide.[3,20] Turning again to the wet chemical method of powder processing it should be pointed out that zirconium forms different ionic species depending on the experimental conditions,[22,23] moreover hydrolysis conditions have a significant influence on crystallization behaviour of precipitated hydrous zirconia subjected to thermal treatment.[23] A detailed study of the influence of hydrogen peroxide on zirconia deposition is in progress and will be reported in due time.

As seen from Fig. 2 the main crystalline phase in region 400–500°C is tetragonal zirconia. However, the size of tetragonal crystallites exceeds the critical value of about 10 nm,[24] as a result transformation to monoclinic phase was observed. The crystallite size of the tetragonal phase at 500°C is higher than that of the monoclinic phase. This result is consistent with Refs 23 and 25. Results of thermal analysis exhibit two steps in weight losses and corresponding endotherms which probably can be attributed to a gradual decomposition of the green deposit to form zirconia. It is in this regard that different stages in weight losses were reported[26] in thermal analysis experiments performed with chemically precipitated zirconia. The exothermic effect at around 460°C is associated with crystallization of zirconia phases and is in agreement with the X-ray data. The crystallization temperature of electrosynthesised zirconia is close to that for the chemically precipitated material.[23,25,26] The results of $ZrTiO_4$ electrodeposition experiments described in previous work[15] showed that the deposit remains amorphous up to 600°C, whereas according to Refs 4 and 14 crystallization of titania and zirconia was observed at ~400°C. However it is reasonable to assume that the crystallization behaviour depends upon electrolyte composition, nature of solvent and substrate. In the light of the above, experimental data should be compared for experiments performed in similar conditions. The results of this work provide such a possibility. Results of X-ray studies show that $ZrTiO_4$ crystallizes directly from the amorphous phase. No peaks of individual components were observed in diffraction patterns obtained at different annealing temperatures. Comparison of X-ray data for deposits 1–3 indicates that crystallization of individual oxides is observed at temperatures at least by 200° lower than the crystallization temperature for zirconium titanate. With this fact in mind, it can be expected that in the case of composition fluctuations in deposit 3, peaks of individual components can be observed. This is especially evident taking into account the nanometric size of zirconia and titania crystallites obtained from stock solutions 1 and 2 respectively.

At this point it is important to note that no exotherms corresponding to crystallization of individual components were detected in the DTA curve for deposit 3. From the results of X-ray studies it can be concluded that the exotherm at ~ 680°C can be attributed to $ZrTiO_4$ crystallization. In this respect, results of Okamoto *et al.*[27] of thermal analysis of titania and zirconia mixtures of different degrees of homogeneity should be mentioned. Remarkably, in the case of composition fluctuations in the mixture of two gels, DTA curves have a quite different behaviour from that for coprecipitated gel, exhibiting additional peaks at temperatures lower than temperature of $ZrTiO_4$ crystallization.[27]

Observed weight losses are associated with the decomposition of the peroxoprecursor. According to the experiments and calculations performed in Ref. 28 the composition of the peroxocompound obtained via the chemical precipitation method was established as $ZrTiO_{3.43}(OH)_{1.13}xH_2O$. According to Ref. 29, the amorphous peroxoprecursor undergoes three structural transformations as the temperature increases. It can be supposed that the steps in weight losses observed in this work correspond to different stages of structural transformations.[29] Going on to Ref. 28 the width of the endothermic peak for deposit 3 around ~130°C can also be attributed to a gradual decomposition of the hydrated peroxide.

On the basis of the above experiments it can be concluded that the temperature of $ZrTiO_4$ formation via electrosynthesis is in agreement with the temperature of formation of this material via the chemical precipitation method.[28,29] It is important to see that the electrodeposynthesis is similar to the wet chemical method of powder processing making use of electrogenerated base instead of alkali. Obviously, electrosynthesis not only produces ceramic materials but also provides their deposition. Going on to Murata *et al.*[30] we can conclude that hydroden peroxide allows us to prevent different hydrolysis rates of individual components and enables us to obtain material of a desired stoichiometry. Hydroxide ions generated in cathodic reactions allows us to perform hydrolysis and obtain colloidal particles near

the cathode. It was supposed[12,15] that the deposition can be achieved via electrophoretic motion of these particles towards the cathode.

Results of this work provide a basis for electrosynthesis of different ferroelectric titanates and solid solutions on Pt substrates, which are important for electronic applications. As an extension of this work recently we have shown the possibility of electrosynthesis of lead zirconate-titanate (PZT) on Pt and on platinized silicon wafers. Results of these studies will be published soon.

5 Conclusions

The feasibility of electrosynthesis of titania, zirconia and zirconium titanate ceramic deposits on platinum substrates has been demonstrated. Obtained materials were found to be amorphous, while their crystallization temperatures are in agreement with those of corresponding powders produced by chemical precipitation methods. The reported data show that the sizes of the obtained crystallites are on a nanometric scale, and their variation with temperature as well as phase evolution has been studied. Results of X-ray studies, thermal analysis and EDS showed that the electrosynthesis of zirconium-titanate via a peroxoprecusor route enables control of its stoichiometry. The obtained results pave the way for the electrodeposition of ferroelectric titanates and their solid solutions.

References

1. Switzer, J. A., Electrochemical Synthesis of Ceramic Films and Powders. *Am. Ceram. Soc. Bull.*, **66** (1987) 1521–4.
2. Zhou, Y., Phillips, R. J. & Switzer, J. A., Electrochemical Synthesis and Sintering of Nanocrystalline Cerium (IV) Oxide Powders. *J. Am. Ceram. Soc.*, **78** (1995) 981–5.
3. Gal-Or, L., Silberman. I. & Chaim, R., Electrolytic ZrO_2 Coatings. I. Electrochemical Aspects. *J. Electrochem. Soc.*, **138** (1991) 1939–42.
4. Chaim., R., Silberman, I. & Gal-Or, L., Electrolytic ZrO_2 Coatings. Microstructural Aspects. *J. Electrochem. Soc.*, **138** (1991) 1942–6.
5. Zhitomirsky, I., Gal-Or, L., Kohn, A. & Hennicke, H. W., Electrochemical Preparation of PbO Films. *J. Mat. Sci. Lett.*, **14** (1995) 807–10.
6. Chaim, R., Stark, G., Gal-Or, L. & Bestgen, H., Electrochemical ZrO_2 and Al_2O_3 Coatings on SiC Substrates. *J. Mat. Sci.*, **29** (1994) 6241–8.
7. Chatterjee, A. P., Mukhopadhyay, A. K., Chakraborty, A. K., Sasmal, R. N. & Lahiri, S. K., Electrodeposition and Characterization of Cuprous Oxide Films. *Mater. Lett.*, **11** (1991) 358–62.
8. Matsumoto, Y., Morikawa, T., Adachi, H. & Hombo, J., A New Preparation Method of Barium Titanate Perovskite Film using Electrochemical Reduction. *Mat. Res. Bull.*, **27** (1992) 1319–27.
9. Matsumoto, Y., Adachi, H. & Hombo, J., New Preparation Method for PZT Films Using Electrochemical Reduction. *J. Am. Ceram. Soc.*, **76** (1993) 769–72.
10. Abolmaali, S. B. & Talbot, J. B., Synthesis of Superconductive Thin Films of $YBa_2Cu_3O_{7-x}$ by a Nonaqueous Electrodeposition Process. *J. Electrochem. Soc.*, **140** (1993) 443–5.
11. Slezak P. & Wieckowski, A., Aqueous Electrochemical Synthesis of $YBa_2Cu_3O_{7-x}$ Superconductors. *J. Electrochem. Soc.*, **138** (1991) 1038–40.
12. Royer P. & Rey, C., Calcium Phosphate Coatings for Orthopaedic Prosthesis. *Surface and Coatings Technology*, **45** (1991) 171–7.
13. Shirkhanzadeh, M., Bioactive Calcium Phosphate Coatings Prepared by Electrodeposition. *J. Mat. Sci. Lett.*, **10** (1991) 1415–17.
14. Zhitomirsky, I., Gal-Or, L., Kohn, A. & Hennicke, H. W., Electrodeposition of Ceramic Films from Non-aqueous and Mixed Solutions. *J. Mat. Sci.*, **30** (1995) 5307–12.
15. Zhitomirsky, I., Gal-Or, L. & Klein, S., Electrolytic Deposition of $ZrTiO_4$ Films. *J. Mat. Sci. Lett.*, **14** (1995) 60–2.
16. Mühlebach, J., Müller, K. & Schwarzenbach, G., The Peroxo Complexes of Titanium. *Inorg. Chem.*, **9** (1970) 2381–90.
17. Hahn, H. & Averback, R. S., Low-Temperature Creep of Nanocrystalline Titanium (IV) Oxide. *J. Am. Ceram. Soc.*, **74** (1991) 2918–21.
18. Siegel, R. W., Ramasamy, S., Hahn, H., Zongquan, L., Ting, L. & Gronsky, R., Synthesis, characterization, and properties of nanophase TiO_2. *J. Mater. Res.*, **3** (1988) 1367–72.
19. Hague, D. C. & Mayo, M. J., The Effect of Crystallization and a Phase Transformation on the Grain Growth of Nanocrystalline Titania. *NanoStruct. Mater.*, **3** (1993) 61–7.
20. Chaim. R., Fabrication and Characterization of Nanocrystalline Oxides by Crystallization of Amorphous Precursors. *NanoStruct. Mater.*, **1** (1992) 479–89.
21. Clark, R. J. H., Bradley, D. C. & Thornton, P., *The Chemistry of Titanium, Zirconium and Hafnium*. Pergamon Press, Oxford, New York, Toronto, 1975, p. 453.
22. Zhang, W. & Glasser F. P., Condensation and Gelation of Inorganic ZrO_2–Al_2O_3 Sols. *J. Mater. Sci.*, **28** (1993) 1129–35.
23. Srinivasan, R., Harris, M. B., Simpson, S. F., De Angelis, R. J. & Davis, B. H., Zirconium Oxide Crystal Phase: The Role of the pH and Time to Attain the Final pH for Precipitation of the Hydrous Oxide. *J. Mater. Res.*, **3** (1988) 787–97.
24. Garvie, R. C. & Goss, M. F., Intrinsic Size Dependence of the Phase Transformation Temperature in Zirconia Microcrystals. *J. Mater. Sci.*, **21** (1986) 1253–7.
25. Mercera, P. D. L., Van Ommen, J. D., Doesburg, E. B. M., Burggraaf, A. J. & Ross J. R. H., Zirconia as a Support for Catalysts. Evolution of the Texture and Structure on Calcination in Air. *Appl. Catal.*, **57** (1990) 127–48.
26. Mercera, P. D. L., Van Ommen, J. G., Doesburg, E. B. M., Burggraaf A. J. & Ross J. R. H., Influence of Ethanol Washing of the Hydrous Precursor on the Textural and Structural Properties of Zirconia. *J. Mater. Sci.*, **27** (1992) 4890–8.
27. Okamoto, Y., Isobe, T. & Senna, M., Mechanochemical Synthesis of Non-crystalline $ZrTiO_4$ Precursor from Inhomogeneous Mixed Gels. *J. Non-Cryst. Solids.*, **180** (1995) 171–9.
28. Navio, J. A., Marchena, F. J., Macias, M., Sanches-Soto, P. J. & Pichat, P., Formation of Zirconium Titanate Powder from a Sol–gel Prepared Reactive Precursor. *J. Mater. Sci.*, **27** (1992) 2463–7.
29. Navio, J. A., Macias, M. & Sanches-Soto, P. J., On the influence of chemical processing in the crystallization behaviour of zirconium titanate materials. *J. Mat. Sci. Lett.*, **11** (1992) 1570–2.
30. Murata, M., Wakino, K., Tanaka, K. & Hamakawa, Y., Chemical preparation of PLZT powder from aqueous solution. *Mat. Res. Bull.*, **11** (1976) 323–8.